Dipartimento di scienze economiche, aziendali, matematiche e statistiche "Bruno de Finetti"

Research Paper Series, N. 2, 2021

An Efficient Monte Carlo Based Approach for the Simulation of Future Annuity Values

Anna Rita Bacinello
Department of Business, Economics, Mathematics and Statistics "B. de Finetti"
University of Trieste, Piazzale Europa 1, 34127 Trieste, Italy

Pietro Millossovich
Department of Business, Economics, Mathematics and Statistics "B. de Finetti"
University of Trieste, Piazzale Europa 1, 34127 Trieste, Italy
Faculty of Actuarial Science and Insurance, The Business School (formerly Cass), City, University of London, 106 Bunhill Row, London EC1Y 8TZ, UK

Fabio Viviano
Department of Business, Economics, Mathematics and Statistics "B. de Finetti"
University of Trieste, Piazzale Europa 1, 34127 Trieste, Italy
Department of Economics and Statistics
University of Udine, Via Tomadini 30/A, 33100 Udine, Italy

UNIVERSITÀ DEGLI STUDI DI TRIESTE

Research Paper Series

Dipartimento di Scienze Economiche, Aziendali, Matematiche e Statistiche
"Bruno de Finetti"
Piazzale Europa 1
34127, Trieste
Tel. +390405587927
Fax +390405587033
http://www.deams.units.it

EUT Edizioni Università di Trieste
Via E.Weiss, 21 - 34128 Trieste
Tel. +390405586183
Fax +390405586185
http://eut.units.it
eut@units.it

ISBN: 978-88-5511-257-4

Research Paper Series, N. 2, 2021

An Efficient Monte Carlo Based Approach for the Simulation of Future Annuity Values

Anna Rita Bacinello
Department of Business, Economics, Mathematics and Statistics "B. de Finetti"
University of Trieste, Piazzale Europa 1, 34127 Trieste, Italy

Pietro Millossovich
Department of Business, Economics, Mathematics and Statistics "B. de Finetti"
University of Trieste, Piazzale Europa 1, 34127 Trieste, Italy
Faculty of Actuarial Science and Insurance, The Business School (formerly Cass), City, University of London, 106 Bunhill Row, London EC1Y 8TZ, UK

Fabio Viviano
Department of Business, Economics, Mathematics and Statistics "B. de Finetti"
University of Trieste, Piazzale Europa 1, 34127 Trieste, Italy
Department of Economics and Statistics
University of Udine, Via Tomadini 30/A, 33100 Udine, Italy

ABSTRACT[1]

In this paper we propose a methodology for valuing future annuity contracts based on the Least-Squares Monte Carlo approach. We adopt, as first step, a simplified computational framework where just one risk factor is taken into account, and then we extend it introducing other sources of risk. We give a brief description of the valuation procedure and provide some numerical illustrations. Furthermore, to test the efficiency of the proposed methodology, we compare our results with those obtained by applying a straightforward and time-consuming approach based on nested simulations. Finally, we present some possible applications in the context of de-risking strategies for pension plans and in the

[1]**Corresponding author:** Pietro Millossovich, email: pietro.millossovich@deams.units.it

valuation of guaranteed annuity options.

KEYWORDS: LSMC, Life annuities, Longevity risk, Stochastic mortality

1. Introduction

Over the 20th century, due to health improvements and medical advances, it has become evident that people tend to live longer and longer. Indeed, the mortality of individuals over time has exhibited many stylized features. In particular, looking at the survival curve for most developed countries around the world, it is immediately clear that mortality levels are decreasing as time passes by, leading to an increase in individual's life expectancy. As a consequence, life insurance companies and pension providers need to face the so-called longevity risk.

The actuarial literature has increasingly focused, in the last decades, on studying and proposing several methods for managing and evaluating this source of risk. The importance of modelling and transferring such a risk is argued in Blake et al. (2013). In particular, it is highlighted how the new longevity-linked capital market instruments could help in facilitating the development of annuity markets and hedging the long-term viability of retirement incomes. As a further consequence, we may recall the non-negligible impact on liabilities of insurers and pension plans, as studied in Oppers et al. (2012).

Recently, some attention has been devoted to the valuation of life annuity contracts issued at a distant future time. This problem has many sources of uncertainty, among which the most relevant are future interest rate and mortality levels. In this regard, Denuit (2008) and Hoedemakers et al. (2005) suggest comonotonic approximations of the life annuity conditional expected present value. Moreover, Cairns (2011), Dowd et al. (2011) and Liu (2013) propose an approach based on a Taylor series approximation of the involved conditional expectation.

The problem of valuing future annuity contracts is getting prominent since it is implicitly present in many contexts such as pricing guaranteed annuity options (GAO) and pension de-risking strategies, i.e. buy-ins and buy-outs. The pricing of GAOs has been faced by many authors (see Ballotta and Haberman, 2003, 2006; Biffis and Millossovich, 2006; Boyle and Hardy, 2003). Concerning the valuation of pension buy-ins and buy-outs, instead, Lin et al. (2017) develop models for pricing both investment and longevity risks embedded in these strategies. Then, Arık et al. (2018) focus in pricing pension buy-outs under dependence between mortality and interest rates. As we will see, facing such a problem requires computing a number of conditional expectations involved in the valuation of annuity contracts at different future times. Hence, avoiding the straightforward and time-consuming approach based on nested simulations would be quite relevant.

For this reason, in this paper we propose a simulation based method to estimate the distribution of future annuity values which is able to strongly decrease the computational demand and at the same time preserves the accuracy of computations. The methodology described in what follows provides an application of the well-established Least-Squares Monte Carlo algorithm (LSMC), originally proposed by Longstaff and Schwartz (2001) for pricing American-type options. The most important advantage of this method is its flexibility to accommodate any type of Markov mortality model, and the possibility to be extended to more complicate frameworks without increasing the complexity of the involved computations. Further, we investigate some variants of the LSMC method in order to improve the accuracy and the robustness of the algorithm. To this end, we exploit the control variates method as suggested by Rasmussen (2005).

The paper is structured as follows. In the next section we introduce the problem under scrutiny and describe our assumptions and the methodology used to solve it, in Section 3 we present a numerical example, and in Section 4 we provide some practical applications. In Section 5, we draw some conclusions.

2. Problem and methodology

The ever-increasing interest on adequately evaluating life insurance products or retirement incomes at a future time relates to the need of providing a reliable valuation of the cost of life expectancy, and to prevent somehow possible insolvency issues. In this paper, our primary goal is to simulate the distribution of the value of an immediate life annuity contract issued to an individual aged $x + T$ at a future time horizon T.

We define the current value at the future time $T > 0$ of a unitary immediate annuity for an individual then aged $x + T$ as

$$a_{x+T}(T) = \sum_{i=1}^{+\infty} B(T, T+i)\, {}_ip_{x+T}\,(T)\,, \tag{1}$$

where $B(T, T+i)$ is the i-th years discount factor prevailing at time $T > 0$ and ${}_ip_y\,(T)$ is the i-th years survival probability for an individual aged y at time T.
The quantities $B(T, T+i)$ and ${}_ip_y(T)$ appearing in Equation (1) are both random variables at time 0 (today), and consequently also $a_{x+T}(T)$ is random. More precisely, these variables are expectations conditional on the information available at time T.

To evaluate these conditional expectations we need models for describing the stochastic evolution of both interest and mortality rates. Under some circumstances, some closed form formulae for computing them are available, for instance when affine processes are used (see Biffis, 2005), but in general this is not guaranteed. As previously mentioned, a straightforward approach would rely on a simulation within simulation procedure, also known as nested simulations; however, since it is quite computationally time-consuming, we are going to propose an application of the LSMC method.

Model framework

In order to evaluate Equation (1), we need to deal with interest and mortality risks. In this Section, we define the computational frameworks which are used to build some numerical results. In a first stage, we assume a stochastic mortality dynamics with a constant interest rate; after, we consider the case in which also the dynamics of interest rates is stochastic.

To this end, we assume to act with a (selected) risk-neutral measure, under which interest and mortality rates are stochastically independent.

Stochastic mortality dynamics

As already discussed, one of the main risk factors affecting the value of an annuity contract is mortality. Hence, we need to adopt a stochastic mortality model in order to mimic its possible evolution over time. To this end, we use the Poisson version of one of the most significant and widely applied stochastic mortality models, i.e. the M7 model (see Cairns et al., 2009). Hence, we assume that the number of deaths at age x and calendar year t, $D_{x;t}$, is Poisson distributed with parameter $E_{x;t}m_{x;t}$, where $E_{x;t}$ and $m_{x;t}$ denote the central exposure and the central death rate, respectively. Moreover, according to Cairns et al. (2009), we assume that the force of mortality is constant over each year of age and calendar and equal to the corresponding central death rate $m_{x;t}$, modelled as

$$\log m_{x;t} = \kappa_t^{(1)} + (x-\bar{x})\kappa_t^{(2)} + \left((x-\bar{x})^2 - \hat{\sigma}_x^2\right)\kappa_t^{(3)} + \gamma_{t-x},$$

where $\bar{x}$ is the average age, $\hat{\sigma}_x^2$ is the average value of $(x-\bar{x})^2$, $\left\{\kappa_t^{(i)}, i=1,2,3\right\}$ are time indexes, and γ_{t-x} accounts for the cohort effect.

Therefore, by exploiting the fact that $\boldsymbol{\kappa}_t = \left\{\kappa_t^{(1)}, \kappa_t^{(2)}, \kappa_t^{(3)}, \gamma_t\right\}$ is usually modelled as a Markov process, we have:

$$_ip_{x+T} = \mathbb{E}\left[\exp\left\{-\left(m_{x+T;T} + \cdots + m_{x+T+i-1;T+i-1}\right)\right\} \mid \boldsymbol{\kappa}_T\right],$$

and, within this framework, we can rewrite Equation (1) as

$$a_{x+T}(T) = \mathbb{E}\left[\sum_{i=1}^{\omega-T-x} \exp\left\{-\left(ir + m_{x+T;T} + \cdots + m_{x+T+i-1;T+i-1}\right)\right\} \mid \boldsymbol{\kappa}_T\right], \tag{2}$$

where ω is the ultimate age and r the constant interest rate.

Stochastic interest rate model

If in a first stage we consider a constant interest rate framework, we then move to extend the complexity of the model by allowing for uncertainty in the future level of the risk-free interest rate.

In this regard, we assume that the interest rate dynamics is described through a CIR process which states that the instantaneous spot interest rate r obeys the following stochastic differential equation

$$dr(t) = \alpha(\bar{r} - r(t))dt + \sigma\sqrt{r(t)}dW(t), \tag{3}$$

where α indicates the strength of the mean reversion process governing r, $\bar{r}$ is the long-term mean instantaneous spot interest rate, σ is the interest-rate volatility parameter, and $W(t)$ is a standard Wiener process.

We know that, under a CIR stochastic interest rate model, the time-T price of a zero-coupon bond with maturity τ, given $r(T)$, is

$$B(T,\tau) = \mathbb{E}\left[e^{-\int_T^{T+t} r(t)dt} \mid r(T)\right] = \exp\{A(\tau-T) - C(\tau-T)r(T)\}, \tag{4}$$

where

$$\begin{aligned}
A(\tau-T) &= \frac{2\alpha\bar{r}}{\sigma^2}\ln\left[\frac{2\gamma e^{(\gamma+\alpha)(\tau-T)/2}}{(\gamma+\alpha)\left(e^{\gamma(\tau-T)}-1\right)+2\gamma}\right],\\
\gamma &= \sqrt{\alpha^2+2\sigma^2},\\
C(\tau-T) &= \frac{2\left(e^{\gamma(\tau-T)}-1\right)}{(\gamma+\alpha)\left(e^{\gamma(\tau-T)}-1\right)+2\gamma}.
\end{aligned}$$

Then Equation (1) can be rewritten as follows

$$a_{x+T}(T) = \mathbb{E}\left[\sum_{i=1}^{\omega-T-x} \exp\left\{-\left(\int_T^{T+i} r(t)dt + m_{x+T;T} + \cdots + m_{x+T+i-1;T+i-1}\right)\right\} \mid r_T, \boldsymbol{\kappa}_T\right]. \qquad (5)$$

The analytic solution in Equation (4) will be used in the construction of the benchmark; specifically, we firstly produce different possible values of $r(T)$ using the SDE in Equation (3), and then we calculate the discount rate through Equation (4). Concerning instead the LSMC algorithm, we will not exploit this analytic solution but the representation of $B(T, \tau)$ in terms of conditional expectation in order to check the reliability of the proposed methodology in a fully simulated framework.

Valuation procedure

The previously introduced framework does not produce a closed form formula for (2), as typically the central death rates have a lognormal distribution so each exponent in (2) involves the sum of lognormal variables. Hence, a possible strategy is to evaluate the involved conditional expectation through simulation based methods.

A straightforward approach would rely on a nested simulations procedure. This strategy requires first to simulate all relevant risk factors up to time T (outer scenarios); then, for each simulated time T value of such factors, one would need to simulate forward starting from that particular value (inner simulations), and finally compute conditional expectations by averaging across all inner simulations. It follows that this method can be computationally expensive, in particular when several annuity values (at different times and/or ages) are needed.

Therefore, in order to reduce the computational complexity, we propose an alternative methodology based on the LSMC approach. It consists on estimating each annuity value at time T by means of a few inner simulations. Obviously, this would lead to biased estimates. Nevertheless, the bias can be reduced by regressing them on a set of basis functions.

Therefore, the LSMC method essentially consists in modelling Equation (1) as a linear combination of basis functions depending on the T-time state vector of the risk factors, $\mathbf{z}_T$. Hence

$$a_{x+T}(T) \approx \tilde{a}_{x+T}(T) = \sum_{j=1}^{M} \beta_j e_j\left(\mathbf{z}_T\right),$$

where $e_j\left(\mathbf{z}_T\right)$ is the j-th basis function in the regression, the β_js represent the coefficients to be estimated, and M is the number of basis functions.

Therefore, the LSMC approach involves two main steps: firstly, we need to perform simulations of the future evolution of the risk factors; then, we use regression across the simulated trajectories in order to obtain estimates of future annuity values. In this way, the conditional expectation is evaluated through regression taking into account the information available at time T (i.e. the simulated values of the state vector $\mathbf{z}_T$ exploited as predictor). Moreover, this method allows to obtain an estimate of the probability distribution of annuity values at future time horizon T for individuals aged $x + T$ at that date. Note that a single set of simulations, without increasing the computational demand, can be used for different ages and time horizons.

3. Numerical results

In this Section we provide some numerical examples by considering two main scenarios: a constant interest rate framework and stochastic mortality evolution, and then we extend the previous model by assuming that also interest rates are stochastic.

Concerning the dynamics of mortality over time, we exploit in both frameworks the M7 mortality model, which has been fitted to the Italian male population data over the period $1965 - 2016$ and ages $35 - 89$ obtained through the Human Mortality Database. Further, we assume that year 2016 corresponds to the evaluation time 0 (today).

To check the accuracy of the estimates, we compare them with those obtained through a nested simulations algorithm, so that the latter act as benchmarks for evaluating the efficiency and the accuracy of the LSMC procedure (see Boyer and Stentoft, 2013).

Constant interest rate framework

In this section, we provide an example based on an immediate life annuity issued to an individual aged 65 at different future time horizons $T \in \{5, 10, 15, 20, 30, 40, 50\}$. The risk-free interest rate is set at the (constant) level $r = 0.03$. Moreover, we simulate a different number of outer trajectories of future mortality $\big($i.e. $n \in \{1000, 5000, 10000, 20000\}\big)$. As basis functions, we use polynomials in three or four variables (depending on whether the cohort term is used or not) with degree $p \in \{1, 2, 3, 4\}$. All the results are then compared with a benchmark obtained through a nested simulations procedure consisting in simulating 20000×20000 scenarios; in total this amounts to 400 millions inner simulations.

Table 1 reports some statistics of the distributions of future annuity values obtained through the two valuation algorithms. Looking at the results, it immediately turns out that, as the time horizon T increases, the distribution changes. Specifically, its mean increases, which is quite reasonable and in line with the ever-increasing life expectancy registered in the last decades. In addition, its standard deviation increases as well, which implies a more dispersed distribution. This result also seems to be reasonable due to the higher uncertainty caused by the longer time horizon. Furthermore, it seems that the distribution tends to be increasingly left-skewed, which implies a longer left tail, hence the distribution is concentrated on the right tail (i.e. higher values of the annuity contract). Finally, we see that the kurtosis increases, meaning that we recognize a heavier tailed distribution, hence a greater propensity to result in extreme annuity values with respect to the Gaussian case.

Table 1. Distribution of annuity values at time horizon T for individuals aged 65 in year $2016+T$. MC 20000×20000 simulations. LSMC 20000×1 simulations, Polynomials order $p = 4$.

		Mean	Std Dev	Skewness	Kurtosis	10th perc.	Median	90th perc.
$T = 5$	MC	13.65110	0.17810	-0.09301	2.96378	13.42178	13.65369	13.87852
	LSMC	13.65221	0.17765	-0.09354	2.94450	13.42258	13.65587	13.87793
$T = 10$	MC	13.85305	0.24099	-0.15187	3.01885	13.54231	13.85969	14.15719
	LSMC	13.85527	0.23900	-0.15067	3.12398	13.54861	13.86207	14.15362
$T = 15$	MC	14.65545	0.27960	-0.23850	3.06219	14.28781	14.66690	15.00814
	LSMC	14.30860	0.26243	-0.19230	3.09234	13.96858	14.31593	14.63883
$T = 20$	MC	14.65545	0.27960	-0.23850	3.06219	14.28781	14.66690	15.00814
	LSMC	14.65588	0.27676	-0.22483	3.12117	14.29383	14.66667	15.00440
$T = 30$	MC	15.42633	0.25877	-0.33438	3.14273	15.08635	15.44058	15.74709
	LSMC	15.42780	0.25820	-0.34241	3.15839	15.08894	15.44244	15.74712
$T = 40$	MC	15.64073	0.29064	-0.41765	3.21743	15.25552	15.66414	15.99685
	LSMC	15.64056	0.28999	-0.41974	3.18686	15.25324	15.66416	15.99541
$T = 50$	MC	15.84853	0.30152	-0.51156	3.33996	15.44801	15.87344	16.21229
	LSMC	15.84871	0.29998	-0.49213	3.28021	15.45142	15.87253	16.21280

Concerning the validation procedure, we can see from Table 1 that the LSMC approach provides quite accurate estimates. Moreover, the reliability of the proposed approach is evidenced by the fact that the obtained distribution overlaps substantially with the one produced through nested simulations; this is also confirmed by the Kolmogorov–Smirnov test (KS, see Table 2). In addition, we have constructed the Q-Q plots by considering the distribution obtained through nested simulations as the theoretical one, and these graphs, once again, confirm the goodness of the proposed method in approaching this kind of problem (see Figure 1).

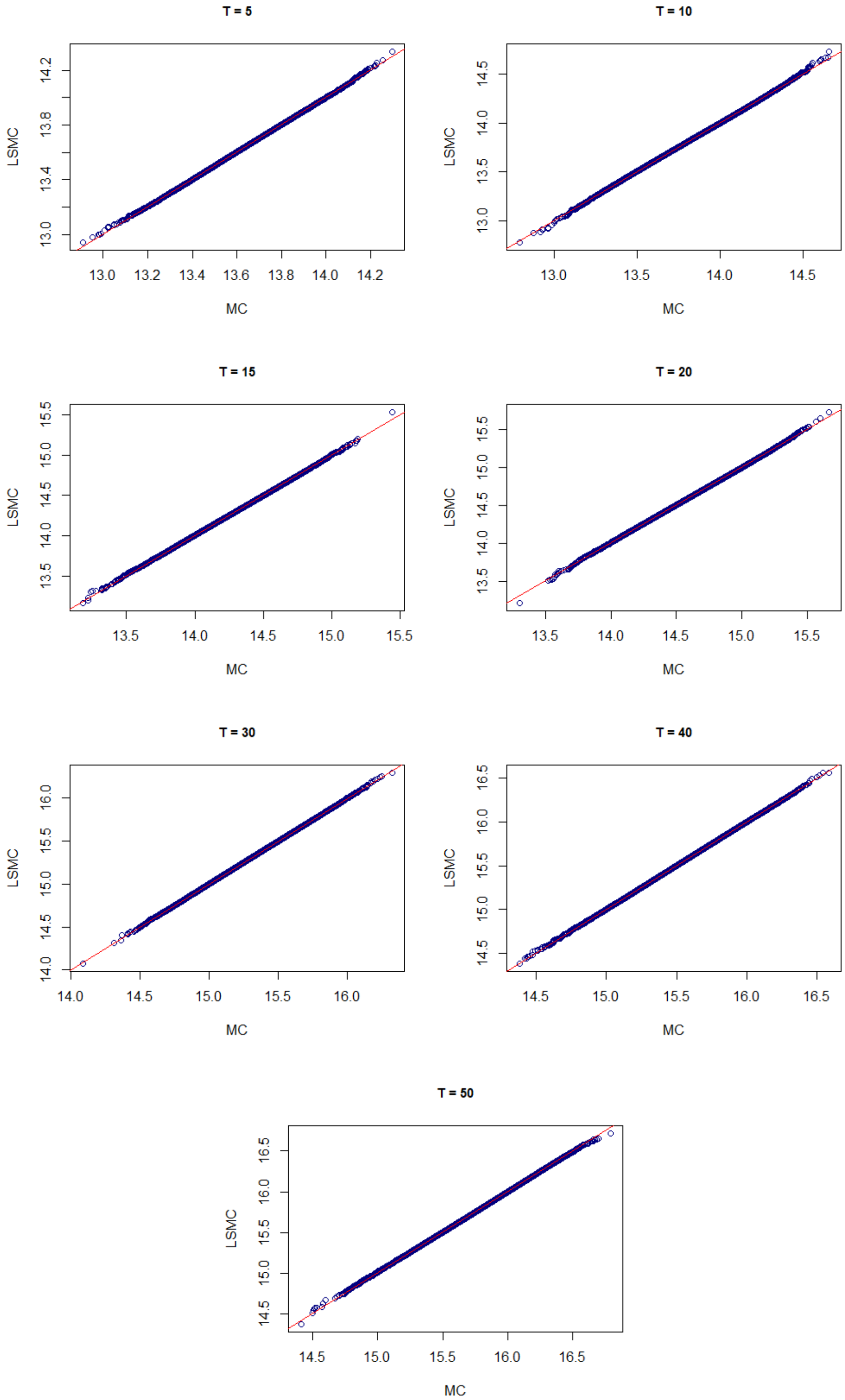

FIG. 1. Q-Q plots of future annuity value distributions for an individual aged 65 at different future times $T \in \{5, 10, 15, 20, 30, 40, 50\}$. MC 20000×20000 simulations; LSMC 20000×1 simulations, Polynomials up to order $p = 4$.

Further, for a more comprehensive analysis, we checked whether the LSMC approach tends to over- or under-estimate the quantities of interest. In this regard, in Table 2 we report the frequency with which the LSMC mean estimates lie inside the 95% confidence interval obtained through the nested simulations procedure or outside (on the left or on the right, respectively). We can see that, in each of the considered scenarios, most of the time the estimates tend to lie outside the confidence interval. Moreover, there is evidence of over-estimation which could be due to biases stemming from the regression.

To improve the accuracy and the stability of the LSMC approach, we may rely on some variance reduction techniques (e.g. control variates or antithetic variates methods) or we may slightly increase the number of inner trajectories. In this regard, Table 3 shows the same quantities already presented in Table 2 obtained by slightly increasing the number of inner trajectories (i.e. 10 inner paths) for each outer level.

Table 2. Frequency of hitting the confidence intervals (columns 1 to 3) and KS Test (columns 4 and 5). MC 20000×20000 simulations. LSMC 20000×1 simulations, Polynomials order $p = 4$.

	Left	Inside	Right	KS Stat. Value	p-value
$T = 5$	20.355%	47.005%	32.640%	0.0056	0.9124
$T = 10$	22.850%	28.460%	48.690%	0.0082	0.5199
$T = 15$	32.775%	28.480%	38.745%	0.0055	0.9228
$T = 20$	34.165%	26.765%	39.070%	0.0048	0.9777
$T = 30$	19.460%	33.265%	47.275%	0.0045	0.9874
$T = 40$	34.475%	28.020%	37.505%	0.0021	1.0000
$T = 50$	35.220%	33.045%	31.735%	0.0026	0.9999

TABLE 3. Frequency of hitting the confidence intervals (columns 1 to 3) and KS Test (columns 4 and 5). MC 20000 × 20000 simulations. LSMC 20000 × 10 simulations, Polynomials order $p = 4$.

	Left	Inside	Right	KS Stat. Value	p-value
$T = 5$	16.195%	72.675%	11.130%	0.00275	1.0000
$T = 10$	17.600%	71.565%	10.835%	0.00235	1.0000
$T = 15$	14.695%	75.845%	9.460%	0.00205	1.0000
$T = 20$	16.210%	73.385%	10.405%	0.00240	1.0000
$T = 30$	16.145%	74.855%	9.000%	0.00185	1.0000
$T = 40$	22.600%	62.665%	14.735%	0.00145	1.0000
$T = 50$	25.470%	55.820%	18.710%	0.00125	1.0000

Concerning the variance reduction techniques, we adopt the control variates method to improve the accuracy of the LSMC approach (see Appendix A for further details). The corresponding results are reported in Table 4.

TABLE 4. Frequency of hitting the confidence intervals (columns 1 to 3) and KS Test (columns 4 and 5). MC 20000×20000 simulations. LSMC with control variates based on 20000×1 simulations and sub-optimal $\theta = -1$, Polynomials order $p = 4$.

	Left	Inside	Right	KS Stat. Value	p-value
$T = 5$	14.590%	65.885%	19.525%	0.0023	1.0000
$T = 10$	12.105%	49.370%	38.525%	0.0052	0.9535
$T = 15$	20.280%	62.655%	17.065%	0.0024	1.0000
$T = 20$	29.130%	46.410%	24.460%	0.0034	0.9999
$T = 30$	11.745%	61.580%	26.675%	0.0031	1.0000
$T = 40$	27.690%	45.510%	26.800%	0.0016	1.0000
$T = 50$	17.335%	55.910%	26.755%	0.0014	1.0000

If we compare Tables 2 and 4, we can see that the control variates technique effectively improves the stability and the accuracy of the LSMC method. However, we can see from Tables 3 and 4 that increasing the number of inner simulations would be more helpful.

Furthermore, we investigate how the choice of the order of polinomials affects the results. For this purpose, we consider polynomials of degree $p \in \{1, 2, 3, 4\}$ and for each of the considered scenarios we perform the KS test in order to measure the statistical distance between the two distributions (LSMC and MC). In particular, Table 5 reports the case of a LSMC algorithm and nested simulations procedure constructed on 20000×1

and 20000×20000 trajectories, respectively.

TABLE 5. KS test statistic value and the corresponding p-value (in brackets) obtained by varying the order of the polynomials and the time horizon T. Results refer to the future annuity value distribution for an individual aged 65 at future time T. LSMC: 20000×1 simulations. MC: 20000×20000.

	Ord. 1	Ord. 2	Ord. 3	Ord. 4
$T = 5$	0.00525 (0.94567)	0.00480 (0.97532)	0.00415 (0.99532)	0.00560 (0.91242)
$T = 10$	0.00745 (0.63559)	0.00605 (0.85759)	0.00775 (0.58530)	0.00815 (0.51994)
$T = 15$	0.01400 (0.03968)	0.00480 (0.97532)	0.00525 (0.94567)	0.00550 (0.92282)
$T = 20$	0.01740 (0.00469)	0.00405 (0.99665)	0.00515 (0.95353)	0.00475 (0.97773)
$T = 30$	0.02125 (0.00024)	0.00365 (0.99935)	0.00405 (0.99665)	0.00450 (0.98741)
$T = 40$	0.03220 (1.973e-09)	0.00155 (1.000)	0.00185 (1.000)	0.00205 (1.000)
$T = 50$	0.03850 (2.669e-13)	0.00240 (1.000)	0.00210 (1.000)	0.00260 (1.000)

If we look at Table 5 by row, we can see that using higher order of polynomials helps to improve the approximation of the desired distribution up to a certain order. The results seem to be totally coherent with the convergence analysis of the LSMC algorithm discussed in Bauer and Ha (2013). Essentially, higher polynomial orders need to be coupled with an increase in the number of simulations in order to achieve better results, see Table 6.

Table 6. KS test statistic value and the corresponding p-value (in brackets) obtained by varying the order of the polynomials and the number of outer simulations. Results refer to the future annuity value distribution for an individual aged 65 at future time $T = 20$. LSMC: $n \times 1$ simulations. MC: 20000×20000 simulations.

	$n = 1000$	$n = 5000$	$n = 10000$	$n = 20000$
Ord. 1	0.04705	0.02435	0.02370	0.01740
	(0.02950)	(0.01742)	(0.00112)	(0.00469)
Ord. 2	0.04495	0.01410	0.00925	0.00405
	(0.04262)	(0.40421)	(0.61832)	(0.99665)
Ord. 3	0.04845	0.01580	0.00870	0.00515
	(0.02287)	(0.27081)	(0.69394)	(0.95353)
Ord. 4	0.05035	0.01575	0.00810	0.00475
	(0.01599)	(0.27422)	(0.77421)	(0.97773)

For a more comprehensive analysis, we perform multiple runs of the LSMC algorithm in order to check the variability of the corresponding estimates. In particular, we run 100 times the LSMC method, by varying both the number of outer scenarios and the future time horizon T. We report in Table 7 the mean absolute percentage error (MAPE) for each scenario computed with respect to the corresponding benchmark value. Figure 2 shows the boxplots relative to the 100 mean estimates obtained through the LSMC approach for an annuity contract issued to an individual aged 65 at the future time $T = 30$.

Table 7. This table illustrates the MAPE of the mean estimates. Each value was computed by considering a sample of 100 estimated measures. The benchmark value is based on a nested simulations algorithm with 20000×20000 simulations. LSMC $n \times 1$ simulations, polynomials order $p = 4$.

	$n = 1000$	$n = 5000$	$n = 10000$	$n = 20000$
$T = 5$	0.0527%	0.0216%	0.0163%	0.0115%
$T = 10$	0.0609%	0.0253%	0.0200%	0.0126%
$T = 15$	0.0621%	0.0285%	0.0221%	0.0179%
$T = 20$	0.0618%	0.0289%	0.0211%	0.0184%
$T = 30$	0.0514%	0.0237%	0.0156%	0.0140%
$T = 40$	0.0576%	0.0304%	0.0240%	0.0234%
$T = 50$	0.0544%	0.0265%	0.0199%	0.0193%

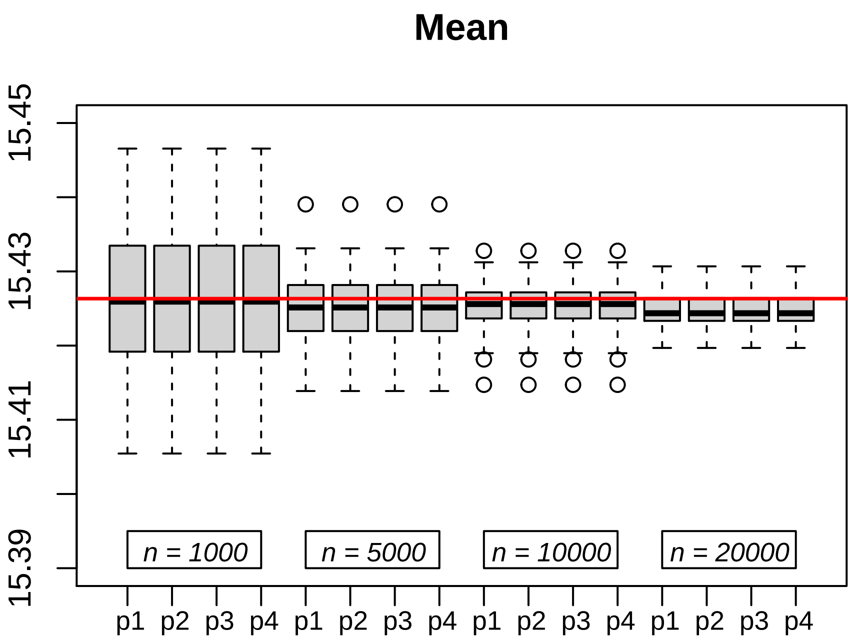

Fig. 2. Box-plots relative to the 100 mean estimates obtained by considering different numbers of outer scenarios and different polynomial orders. Age 65 at time $T = 30$. LSMC $n \times 1$ simulations, varying polynomial orders p. The red line is the benchmark value based on 20000×20000 simulations.

As we can see from Table 7 and Figure 2, increasing the simulated outer scenarios helps the LSMC algorithm to converge. In addition, looking at Figure 2, it seems that, if the number of simulations is taken fixed, the choice of the polynomial order does not affect the reliability of the desired quantity at least for the mean estimate of the distribution. However, we may be interested in analysing the performance of the LSMC in estimating some extreme values of the distribution. In this regard, we present in Table 8 and Figure 3 the MAPE and box-plots relative to the 90-th percentile estimates for an immediate life annuity issued to an individual aged 65 at time $T = 30$, respectively. Once again, each box-plot was generated by considering 100 estimates, by varying the number of outer simulations and the order of the polynomials.

Table 8. MAPE of the 90-th percentile estimates computed with the LSMC method for the immediate life annuity issued to an individual aged 65 at time $T = 30$ by varying the number of outer simulations n and the polynomial order $p \in \{1, 2, 3, 4\}$. Each value was computed by considering a sample of 100 estimated percentiles. Benchmark value based on 20000×20000 simulations.

	Ord. 1	Ord. 2	Ord. 3	Ord. 4
$n = 1000$	0.1010%	0.0682%	0.0688%	0.0738%
$n = 5000$	0.0893%	0.0371%	0.0366%	0.0371%
$n = 10000$	0.0875%	0.0329%	0.0306%	0.0308%
$n = 20000$	0.0842%	0.0245%	0.0230%	0.0229%

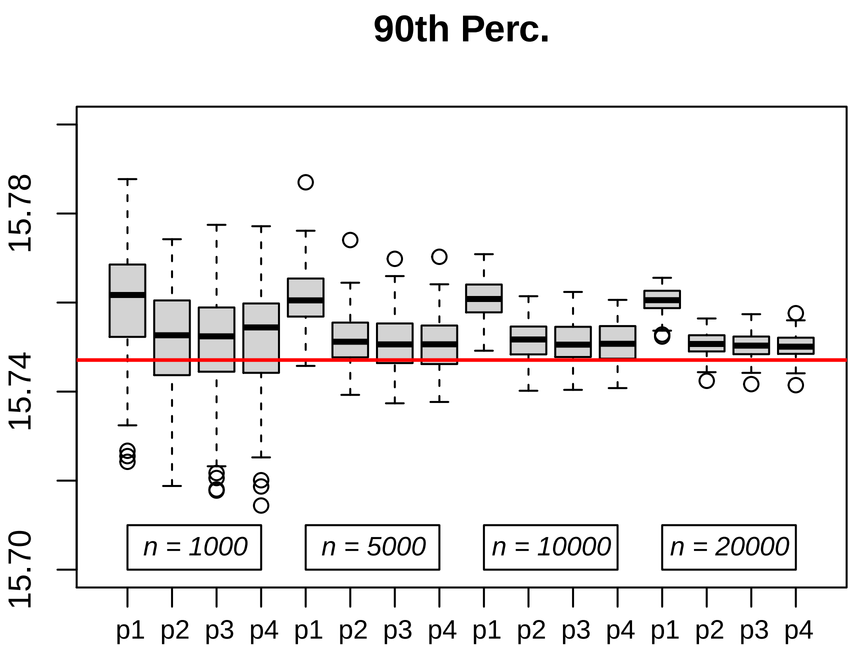

Fig. 3. Box-plots relative to the 90-th percentile estimates of the immediate life annuity distribution issued to an individual aged 65 at time $T = 30$. Each box-plot was generated by considering 100 estimates by varying the number of simulations n and the order of the involved polynomials. The red line corresponds to the 90-th percentile estimate obtained through nested simulations (20000×20000).

From Table 8 and Figure 3, it is evident that, for higher number of simulations, we need to exploit higher polynomial orders. Indeed, we can see from Table 8 that, by simulating 1000 trajectories, it is sufficient to use a lower polynomial order (i.e. $p = 2$); instead, once we increase the simulated trajectories, then we need to increase at the same time p. Moreover, by looking at Figure 3, it seems that the LSMC approach tends to overestimate the desidered quantity in all the scenarios. However, the magnitude of such overestimation is quite negligible (see Table 8).

Note that we can exploit as basis functions other types of polynomials. For instance, we have conducted a similar analysis by using the so-called orthogonal polynomials (such as Hermite, Legendre, Laguerre and Chebyshev). However, here we do not report the corresponding results since they turned out to be quite similar to the previously discussed and hence, at least in this simplified framework, they do not provide any significant improvement.

Finally, in Figure 4 we compare the accuracy of the LSMC method with and without control variates and the LSMC approach with a greater number of inner scenarios. In particular, Figure 4 shows the MAPEs relative to the mean and the 90-th percentile estimates obtained by varying the number of outer trajectories.

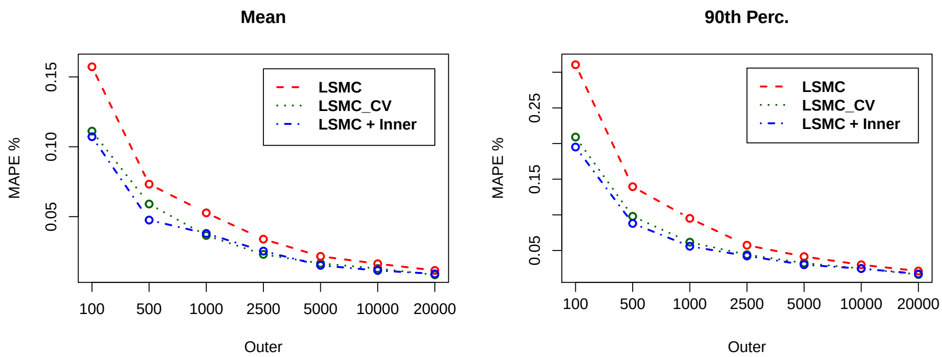

FIG. 4. MAPEs relative to the mean (left) and the 90-th percentile (right) estimates of the immediate life annuity distribution issued to an individual aged 65 at time $T = 5$ obtained by running 100 times the LSMC method (LSMC), the LSMC approach with control variates (LSMC_CV), and the LSMC method with 10 inner trajectories. Monomials up to order $p = 4$ have been employed. Benchmark values based on 20000×20000 simulations.

As we can see from Figure 4, as the number of outer simulations increases, the level of accuracy of the three algorithms converges. In addition, we can see that applying the control variates technique or increasing the number of inner trajectories produces similar results in terms of accuracy in each of the considered cases. We have conducted a similar analysis by varying the future time horizon T, and we have obtained similar outcomes.

Now let us examine the speed of the LSMC algorithm and the nested simulations one. Table 9 shows the runtime of the two approaches for different numbers of outer simulations and a specific time horizon (i.e. $T = 20$). Note that we conducted all experiments using a custom-built workstation equipped with an Intel® Xeon® Silver 4116CPU 2.10 GHz processor with 64 GB of RAM and Windows 10 Pro for Workstation operating system.

Table 9. Time in seconds demanded by the two approaches. MC based on $n \times 20000$ simulations. LSMC based on $n \times 1$ simulations, Polynomials order $p = 4$. Individual aged 65 at time $T = 20$.

	$n = 1000$	$n = 5000$	$n = 10000$	$n = 20000$
LSMC	16.23	74.45	148.53	294.00
MC	274.58	1350.07	2784.07	5564.53
LSMC / MC	5.91%	5.52%	5.34%	5.28%

From Table 9, we can appreciate in each of the considered scenarios how the LSMC outperforms the nested simulation method. In addition, as we have seen, one possible choice to improve the accuracy of the results would be to slightly increase the number of inner trajectories employed in the LSMC setting (see Table 3). For this reason, in Table 10 we investigate in terms of time the cost of such a procedure.

Table 10. Time in seconds demanded by the LSMC method based on $n \times 1$ and $n \times 10$ simulations. Polynomials order $p = 4$. Individual aged 65 at time $T = 20$.

Inner	$n = 1000$	$n = 5000$	$n = 10000$	$n = 20000$
1	16.23	74.45	148.53	294.00
10	20.89	97.21	195.04	394.10
1 / 10	77.69%	76.59%	76.17%	74.62%

We can see from Table 10 that increasing the inner scenarios from 1 to 10, as expected, leads to an increase in the computational time (e.g. it costs around 25% more).

Stochastic interest rate framework

In this Section, we provide numerical examples on the estimation of future annuity values by considering the two main risk factors affecting the value of the policy under scrutiny, e.g. future mortality and interest rate levels. For this purpose, we assume that the interest rate dynamics is described by a CIR process (see Section 2), while the evolution of mortality is still described through the M7 mortality model. We set the parameters entering the SDE in Equation (3) as follows: $r_0 = 0.04$, $\alpha = 0.2$, $\bar{r} = 0.04$ and $\sigma = 0.1$, as in Dowd et al. (2011). Again, we consider an annuity contract which will be issued to an individual aged 65 at different future times $T \in \{5, 10, 15, 20, 30\}$.

We simulate $n \in \{1000, 5000, 10000, 20000\}$ outer scenarios both for mortality and interest rates (assuming independence among the two sources of uncertainty). As already said, the nested simulations approach exploits the analytic solution in Equation (4) while the LSMC method is constructed on a fully simulated scenario based on an Euler discretization setting for the SDE in Equation (3).

Focusing on our proposed methodology, we consider as basis functions employed in the regression model polynomials with different order $p \in \{1, 2, 3, 4\}$. Table 11 reports summary statistics about the obtained distributions of future annuity values by considering an individual aged 65 at different future times T and applying both the nested simulation and the LSMC approaches. Figure 5 shows the probability density functions of the annuity contract value issued to an individual aged 65 at the future time $T = 30$ obtained by the two methodologies.

TABLE 11. Distribution of annuity values at time horizon T for individuals aged 65 in year $2016+T$. MC 20000×20000 simulations. LSMC 20000×1 simulations, Polynomials order up to $p = 4$.

		Mean	Std Dev	Skewness	Kurtosis	10th perc.	Median	90th perc.
$T = 5$	MC	12.72846	1.29133	-0.74746	3.42607	10.92840	12.93567	14.20394
	LSMC	12.74919	1.32597	-0.80183	3.67530	10.92036	12.96490	14.24625
$T = 10$	MC	12.91861	1.36829	-0.90133	3.93803	11.04426	13.16814	14.42813
	LSMC	12.94864	1.39122	-0.86954	4.01465	11.06078	13.17963	14.49531
$T = 15$	MC	13.32751	1.42048	-0.90174	3.99626	11.38111	13.58073	14.89697
	LSMC	13.36619	1.44427	-0.86384	4.04043	11.40266	13.60434	14.97452
$T = 20$	MC	13.65274	1.45657	-0.89477	3.93755	11.64542	13.90389	15.27137
	LSMC	13.66774	1.49907	-0.90988	3.98496	11.58720	13.93839	15.31676
$T = 30$	MC	14.31109	1.54101	-0.91214	4.00030	12.21987	14.59021	16.01540
	LSMC	14.31839	1.58931	-0.87445	3.95985	12.15367	14.59332	16.09910

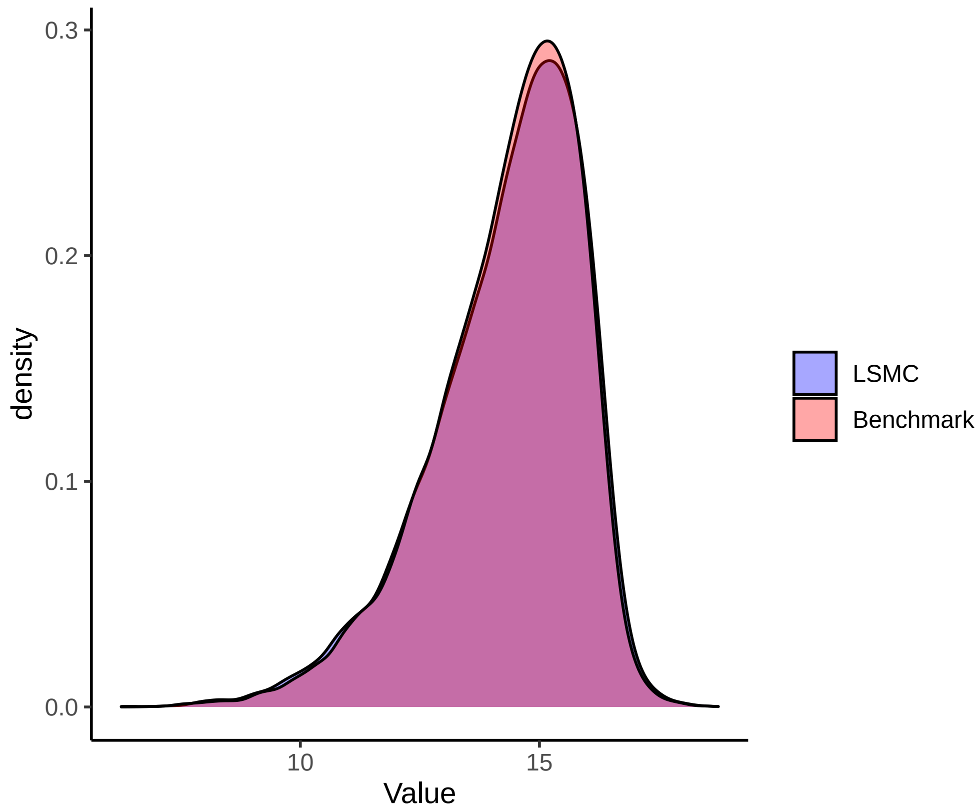

Fig. 5. Probability density function relatives to future annuity values issued to an individual aged 65 at future time $T = 30$ under stochastic interest rate and mortality framework. LSMC 20000×1 simulations, Polynomial order $p = 2$. Benchmark based on 20000×20000 simulations.

Once again, we can appreciate the reliability of the proposed methodology. Further, as already recognized in Dowd et al. (2011), incorporating interest rate risk makes the distribution much more left-skewed. In Table 12 we report the MAPEs relative to the mean estimates obtained by running 100 times the LSMC algorithm. We can see that, compared to Table 7, the accuracy gets worst. This is obviously due to the increasing uncertainty in the valuation process given by the stochastic evolution of the risk-free rate. Nonetheless, the LSMC method is still able to provide reliable estimates, especially if we increase the number of outer scenarios.

TABLE 12. This table illustrates the MAPE of the mean estimates. Each value was computed by considering a sample of 100 estimated measures. The benchmark value is based on a nested simulations algorithm with 20000 $\times$ 20000 simulations. LSMC $n \times 1$ simulations, polynomials order $p = 4$.

	$n = 1000$	$n = 5000$	$n = 10000$	$n = 20000$
$T = 5$	0.4840%	0.1417%	0.1134%	0.0979%
$T = 10$	0.3414%	0.2594%	0.1167%	0.0957%
$T = 15$	0.3519%	0.1409%	0.2236%	0.0997%
$T = 20$	0.3470%	0.1718%	0.1051%	0.1040%
$T = 30$	0.3499%	0.2399%	0.1683%	0.1044%

Also in this case we investigate the accuracy of the LSMC in approximating extreme values of the distribution. In this regard, Table 13 and Figure 6 show the MAPEs and the boxplots relative to the 90-th percentile estimates obtained by performing 100 times the LSMC approach (for different polynomial orders and number of simulations). As we can see, in this case lower polynomial orders are already sufficient to provide a good performance. This is in line with the theory since in this framework we are considering one more risk-factor entering as predictor in the regression model, i.e. the interest rate $r(T)$ [2].

TABLE 13. MAPE of the 90-th percentile estimates computed with the LSMC method for the immediate life annuity issued to an individual aged 65 at time $T = 30$ by varying the number of outer simulations n and the polynomial order $p \in \{1, 2, 3, 4\}$. Each value was computed by considering a sample of 100 estimated percentiles. Benchmark value based on 20000 $\times$ 20000 simulations.

	Ord. 1	Ord. 2	Ord. 3	Ord. 4
$n = 1000$	0.6272%	0.5690%	0.6555%	0.7313%
$n = 5000$	0.3851%	0.5876%	0.6655%	0.6950%
$n = 10000$	0.3214%	0.5655%	0.6472%	0.6562%
$n = 20000$	0.5415%	0.3473%	0.4067%	0.4108%

[2] If we considered a polynomial order $p = 1$ or $p = 2$ and, as in this case, we have 4 risk-factors $\left(\kappa_T^{(1)}, \kappa_T^{(2)}, \kappa_T^{(3)}, r_T\right)$, then the number of basis functions would be $M = 5$ and $M = 15$, respectively.

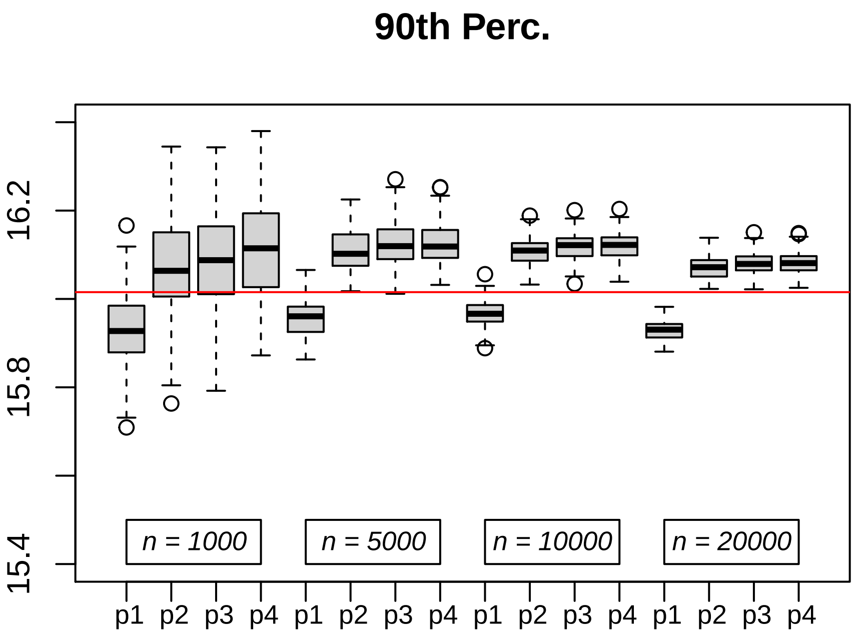

Fig. 6. Box-plots relative to the 90-th percentile estimates of the immediate life annuity distribution issued to an individual aged 65 at time $T = 30$ under stochastic interest rate and mortality. Each box-plot was generated by considering 100 estimates by varying the number of simulations n and the order of the involved polynomials. The red line corresponds to the 90-th percentile estimate obtained through nested simulations 20000×20000.

4. Applications

In this last part of the paper, we present some possible applications in which the valuation of future annuity contracts plays a relevant role, and hence where our proposed methodology helps in strongly reducing the computational time, while simultaneously ensuring a high reliability.

As already mentioned in Section 1, the problem of valuing future annuity contracts recurs in various contexts, e.g. in developing de-risking strategies for pension providers, or in predicting their pension shortfall distribution in a future time horizon, or for pricing purposes such as valuing Guaranteed Annuity Options, just to name a few. In this regard, the next sections provide numerical applications of the LSMC method in addressing these issues.

Pricing pension buy-outs

In this Section, we apply the LSMC methodology for pricing de-risking strategies; in particular, we focus on pricing pension buy-outs.

In the case of a buy-out, a pension provider transfers part of its assets and pension liabilities to an insurance company which plays as contractual counterparty. The latter requires the payment of an amount equal to the actuarial expected present value of possible future pension plan's deficit. In the following, we introduce a simplified computational framework.

Let us consider a pension plan based on a cohort of pensioners N_0 at year $t = 0$ with age x_0. Further, we assume that all pensioners receive the same constant pension benefit, b, at the end of each year, if alive. We indicate with L_t the pension liability at year t, which is given by

$$L_t = N_t \cdot b \cdot a_{x_0+t}(t), \tag{6}$$

where N_t is the number of survivors at the calendar year t, and $a_{x_0+t}(t)$ is the value of an ordinary annuity contract issued to an individual aged $x_0 + t$ in year t (with unitary benefits), see Equations (1) and (2) in Section 2. Then, we denote with A_t the value of the pension assets in year t.

At the end of each year, the pension plan must pay the benefits to the survivors, implying a reduction of the pension portfolio value. In case that the portfolio itself is not able to cover such payments, the pension buy-out option obliges the insurer to cover the remaining amount. Therefore, we define such amount as O_t, which can be formalized as follows:

$$O_t = \max\{L_t + N_t \cdot b - A_t \ , \ 0\} \quad t = 1, 2, \dots .$$

Obviously, just after the pensions are paid, the value of the pension portfolio can be expressed as

$$A_{t+} = A_t - N_t \cdot b + O_t = \max\{A_t - N_t \cdot b \ , \ L_t\} \quad t = 1, 2, \dots,$$

which will be then re-invested between times t and $t + 1$.

Therefore, under this setting, we can define the risk-neutral price of the funding guarantee option of the buy-outs as

$$G = \mathbb{E}\left[\sum_{t=1}^{\tau} e^{-rt} O_t - e^{-r(\tau+1)} A_{\tau+1}\right], \tag{7}$$

where $\tau = \max\{t : N_t > 0\}$ and, again, we have assumed a constant risk-free interest rate, r. In addition, the price G can be decomposed in two components

$$G = G_O - G_A,$$

where

$$G_O = \sum_{t=1}^{\tau} e^{-rt} \cdot \mathbb{E}[O_t],$$
$$G_A = e^{-r(\tau+1)} \cdot \mathbb{E}[A_{\tau+1}].$$

Hence, G_O can be interpreted as the actuarial present value of the future contributions made by the insurer in order to compensate the deficit; and G_A as the present value of the assets, once the cohort becomes extinct, which will be ceeded to the insurer. The premium in Equation (7) can also be defined as a percentage of the value of the pension liabilities at time $t = 0$, i.e.

$$g = \frac{G}{L_0} = \frac{G_O}{L_0} - \frac{G_A}{L_0} = g_O - g_A.$$

Numerical results

Concerning the dynamics of mortality, in order to take into account the difference in terms of longevity between the target population and that of the retired cohort, we exploit the Augmented Common Factor mortality model proposed in Li and Lee (2005). Indeed, in practice, if the value of future annuity contracts in Equation (6) are derived from a reference population, the number of survivors N_t instead reflects the mortality evolution of the specific retired cohort belonging to the pension plan. Therefore, we consider as reference population the italian total one, and we assume that the pension plan consists of female italian retirees. We exploit data over the period 1960-2016 and range of ages $65 - 89$ obtained from the Human Mortality Database.

Concerning the dynamics of the pension portfolio, for simplicity we assume that A_t follows a Geometric Brownian Motion with drift equal to the risk-free rate $r = 0.02$, and volatility $\sigma_A \in \{0, 0.05, 0.10, 0.15, 0.20\}$. Moreover, we assume that at time $t = 0$ the pension plan is fully funded, i.e. $A_0 = L_0 = 172299$.

We assume that at time $t = 0$ the pension plan signs a pension buy-out contract for the cohort of $N_0 = 10000$ female pensioners all aged $x_0 = 65$ at that time, and we fix as ultimate age $\omega = 110$, i.e. $\omega - x_0 = 45$. The mortality table is completed up to the ultimate age through a log-linear closure.

In order to evaluate Equation (7), we firstly need to evaluate Equation (6) which depends on the value of future annuity contracts. For this purpose, we apply the LSMC methodology based on a set of 100000×1 scenarios of mortality rates. Then, concerning the regression part of the algorithm, we exploit polynomials up to order $p \in \{1, 2\}$.

In Tables 14 and 15 we report the value at time $t = 0$ of a pension buy-out obtained through the LSMC approach for different values of σ_A and by varying p.

Table 14. Price of a pension buy-out contract at time $t = 0$ obtained by varying the level of volatility σ_A. LSMC 100000×1 simulations, Polynomials up to order $p = 1$.

σ_A	g_O	g
0	5.266%	4.561%
0.05	12.010%	4.590%
0.10	22.497%	4.700%
0.15	34.145%	4.968%
0.20	46.858%	5.529%

Table 15. Price of a pension buy-out contract at time $t = 0$ obtained by varying the level of volatility σ_A. LSMC 100000×1 simulations, Polynomials up to order $p = 2$.

σ_A	g_O	g
0	5.261%	4.561%
0.05	12.009%	4.590%
0.10	22.497%	4.700%
0.15	34.145%	4.969%
0.20	46.858%	5.529%

As we can notice from Tables 14 and 15, the higher σ_A the higher the pension buy-out price. Moreover, we can see that the choice of the polynomial order has not a relevant effect on g; similar results were obtained by exploiting higher polynomial orders.

We have reported just a simple numerical application which gives an idea of the potentiality of the LSMC method. Indeed, the approach drastically reduces the computational time which would be required if a simulation within simulation approach is used. Indeed, addressing this problem implies the valuation of a sequence of future annuity contracts (for instance, in this case we need estimates of $a_{x_0+t}(t)$ for $t = 1, \ldots, \omega - x_0$). Specifically, the computational budget passes from $100000 \times 100000 \times (\omega - x_0)$ simulations in case of nested simulations to $100000 \times 1 \times (\omega - x_0)$ in the LSMC setting.

Pension shortfall

As a further application, we may be interested in approximating the shortfall distribution for a pension provider in a distant future time T, which would be essential for solvency capital valuations. In this regard, we exploit the same framework introduced in the previous subsections to approximate the shortfall distribution at time $T = 1$ year, but instead of a female retirees cohort a male one is taken into account. In particular, we define the pension shortfall after 1 year and discounted at time $t = 0$ as

$$S = e^{-r} \left[L_1 - A_{1+} \right] = e^{-r} \left[N_1 \cdot b \cdot a_{x_0+1}(1) - A_{1+} \right], \tag{8}$$

again with $r = 0.02$, L_1 denotes the pension liabilities at time $t = 1$, and A_{1+} is the pension portfolio value just after the pensions are paid at the end of the first year.

In order to evaluate Equation (8), we need to work under two probability measures. A physical (or real-world) probability measure $\mathbb{P}$ over the first year to simulate the possible evolution of the relevant risk-factors; and the risk-neutral probability measure over the remaining time horizion (up to the last date in which the pension plan has survivors). In particular, looking at Equation (8), the number of survivors and the value of the pension assets at time $t = 1$ should be valued under $\mathbb{P}$, while $a_{x_0+1}(1)$ under the risk-neutral measure. In this regard, we assume now to start from the dynamics of mortality under the physical measure $\mathbb{P}$ and, to obtain that under the risk-neutral measure, we apply the valuation method suggested in Wang (2000) (see Appendix B for details).

The exploited mortality data are those already used in the previous subsection. Moreover, we assume that, under $\mathbb{P}$, the pension portfolio value evolves according to a GBM with constant drift $\mu = 0.08$ and volatility $\sigma_A \in \{0.05, 0.10, 0.20\}$. The hypothesis that the pension plan is fully funded at the initial time is still valid.

We simulate $n = 100000$ $\mathbb{P}$-trajectories of the risk-factors up to time $t = 1$, and then we project just 1 inner scenario to which is applied the Wang Transform. The LSMC method is then applied in order to evaluate $a_{66}(1)$, by exploiting polynomials up to order $p \in \{1, 2, 3\}$.

We investigate the 1-year shortfall distribution for different values of the longevity risk premium $\lambda \in \{0.0456849, 0.1320511, 0.2209899\}$ which were obtained by setting different values for $a_{65}(0)$[3]. For each scenario, we estimate the corresponding Value-at-Risk (VaR) and Conditional Value-at-Risk (CVaR) at the 99.5-th level, which are usually used for valuing solvency capital requirements.

Table 16 reports the $\text{VaR}_{99.5\%}$ and $\text{CVaR}_{99.5\%}$ of the 1-year shortfall distribution discounted at time $t = 0$ (see Figure 7) expressed as percentage of the initial pension liabilities value $L_0 = 172299$, obtained by varying the longevity risk premium λ and the pension portfolio volatility σ_A.

[3]The longevity risk premium were obtained by setting $a_{65}(0) = \{17.5, 18, 18.5\}$.

TABLE 16. This table reports the 99.5% VaR and CVaR estimates of the pension shortfall distribution after 1 year, discounted at time $t = 0$, as a percentage of the initial level of the pension liabilities for different values of the longevity risk premium λ, different polynomial order p, and volatility levels σ_A. Note that $L_0 = 172299$.

		$\lambda = 0.0456849$		$\lambda = 0.1320511$		$\lambda = 0.2209899$	
p	σ_A	$\text{VaR}_{99.5\%}$	$\text{CVaR}_{99.5\%}$	$\text{VaR}_{99.5\%}$	$\text{CVaR}_{99.5\%}$	$\text{VaR}_{99.5\%}$	$\text{CVaR}_{99.5\%}$
1	0.05	9.210%	10.777%	14.138%	15.715%	18.986%	20.581%
	0.10	20.587%	23.292%	25.555%	28.236%	30.434%	33.110%
	0.20	39.936%	43.901%	44.872%	48.849%	49.752%	53.728%
2	0.05	9.213%	10.778%	14.145%	15.716%	18.985%	20.582%
	0.10	20.593%	23.292%	25.561%	28.236%	30.437%	33.110%
	0.20	39.935%	43.901%	44.890%	48.850%	49.766%	53.729%
3	0.05	9.214%	10.779%	14.143%	15.717%	18.985%	20.583%
	0.10	20.591%	23.292%	25.558%	28.237%	30.435%	33.110%
	0.20	39.932%	43.901%	44.893%	48.850%	49.769%	53.729%

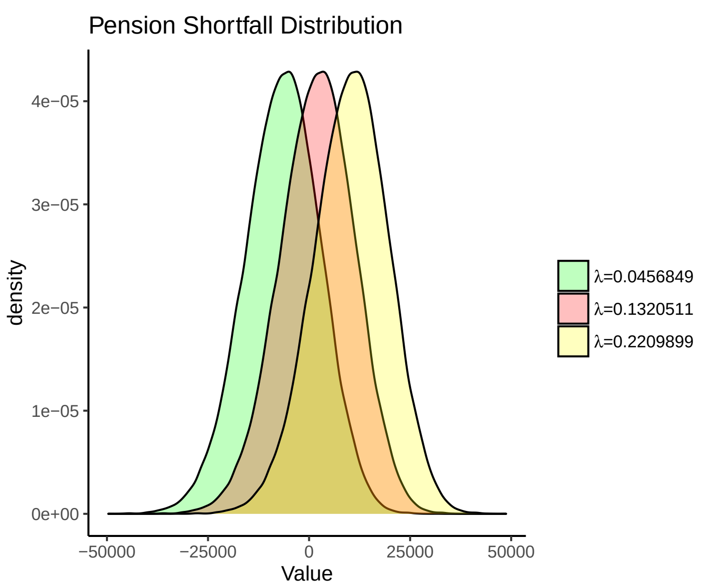

FIG. 7. Distribution of the pension shortfall after 1 year discounted at time $t = 0$ by considering different levels of the longevity risk premium λ. LSMC 100000×1, Monomials order $p = 1$. $\sigma_A = 0.05$.

As we can see from Table 16, an increase in the volatility σ_A as well as in the longevity risk premium λ (i.e. increasing life expectancy) imply higher levels for both VaR and CVaR; this is quite reasonable since an unexpected increase in longevity leads to higher possible losses for pension sponsors. In addition, changing the polynomial order in the LSMC algorithm does not particularly affect the results.

Pricing Guaranteed Annuity Options

In this Section, we present a further context where future annuity contract values are needed, and so where our proposed methodology could be applied. In particular, we focus on estimating the price of a future Guaranteed Annuity Option contract. In addition, we remind the readers to consult Ballotta and Haberman (2003, 2006), Boyle and Hardy (2003), and Biffis and Millossovich (2006) for deeper details.

Description

A guaranteed annuity option (GAO) is a contract that provides the policyholder the right to convert a specific amount at maturity (e.g. benefits embedded in unit-linked policies) into a life annuity at some guaranteed conversion rate, c (fixed at inception). In particular, the option is exercised at maturity if the future annuity value prevailing in the market is greater then the guaranteed annuity (the reciprocal of the conversion rate, c) granted by the insurer at inception.

Let us consider a policyholder aged x years at the inception date $t = 0$. We assume that the amount available at maturity, i.e. at time $T > 0$, is given by the value of a reference fund with price process S, and that the guaranteed conversion rate $0 < c < 1$ is fixed at inception. Then, the time-0 value of a GAO with maturity T can be expressed as

$$V_0 = \mathbb{E}\left[e^{-\int_0^T (r_s+\mu_{x+s})ds} cS_T \max\left\{a_{x+T}(T) - \frac{1}{c}, 0\right\}\right], \tag{9}$$

where S_T is the account value at time T which can be converted into an annuity. Therefore, as we can see from Equation (9), a Guaranteed Annuity Option can be interpreted as a call option on the annuity value, and the strike is the reciprocal of the guaranteed conversion rate. We refer to Biffis and Millossovich (2006) for deeper details.

Numerical results

The computational framework is the same as the one introduced in Section 3, hence we exploit a CIR process and the M7 model for simulating the dynamics of interest rates and mortality over time, respectively.

In our numerical example, we consider diffent individuals aged $x < 65$ in 2016 ($t = 0$), and that the GAO matures when they reach age $x + T = 65$; at that time they can choose to convert the account value $S_T = 100$ into annuities at the conversion rate $c = \frac{1}{13}$. Therefore, just for simplicity and without loss of generality, we ignore the dynamics of a hypothetical reference fund.

The LSMC method is then applied to estimate the value of a future annuity contract which enters in Equation (9), by performing $n \times 1$ simulations of the risk-factors and by exploiting polynomials up to order $p \in \{1, 2, 3, 4\}$. In this case, we compare these results with respect to the corresponding benchmark based on nested simulations (20000×20000 trajectories). Table 17 reports the price of a GAO for an individual aged x today with maturity T together with the probability that the option ends in-the-money, obtained by both the LSMC and the simulation within simulation algorithms.

TABLE 17. This table reports the price of a Guaranteed Annuity Option with maturity T for an individual aged x today together with the probability that the option ends in-the-money. The values are computed both by exploiting the LSMC approach for the evaluation of the future annuity contracts, and the nested simulations procedure. The LSMC method is based on 20000×1 simulations of the risk factors, polynomials with order $p = 1$. Nested simulations based on 20000×20000 scenarios.

x	60	55	50	45	35
T	5	10	15	20	30
V_0^{LSMC}	2.362	2.594	3.382	3.666	3.970
$\Pr\left[a_{x+T}(T) > \frac{1}{c}\right]_{LSMC}$	0.515	0.578	0.684	0.740	0.830
V_0^{MC}	2.353	2.594	3.315	3.614	3.923
$\Pr\left[a_{x+T}(T) > \frac{1}{c}\right]_{MC}$	0.480	0.547	0.651	0.716	0.816

As we can see from Table 17, the LSMC method provides quite accurate estimates; indeed, the mean percentage error among all the prices is around 1%. This result is quite notable since the nested simulations approach exploits the closed formula in Equation (4), while the LSMC algorithm is based on a fully simulated framework bringing with itself all the errors related to the discretization of the interest rate stochastic process.

Moreover, we investigate the accuracy of the LSMC method by performing multiple runs, varying both the number of outer scenarios, n, and the polynomial order, p. In this regard, Table 18 and Figure 8 report the MAPEs and box-plots relative to the GAO price estimates obtained by running 100 times the LSMC and compared to the corresponding benchmark based on 20000×20000 simulations. The results refer to a GAO subscribed by an individual aged $x = 55$ today and maturity $T = 10$.

TABLE 18. This table illustrates the MAPE of the GAO price estimates obtained by performing 100 runs of the LSMC method by varying both the number of outer scenarios and the polyinomial order. The benchmark value is based on a nested simulations algorithm with 20000 × 20000 simulations. GAO subscribed by an individual aged $x = 55$ today with maturity $T = 10$.

n	$p = 1$	$p = 2$	$p = 3$	$p = 4$
1000	5.009%	7.143%	7.936%	9.435%
5000	2.736%	5.952%	6.179%	6.447%
10000	1.763%	4.827%	4.938%	4.968%
20000	1.464%	4.589%	4.673%	4.684%

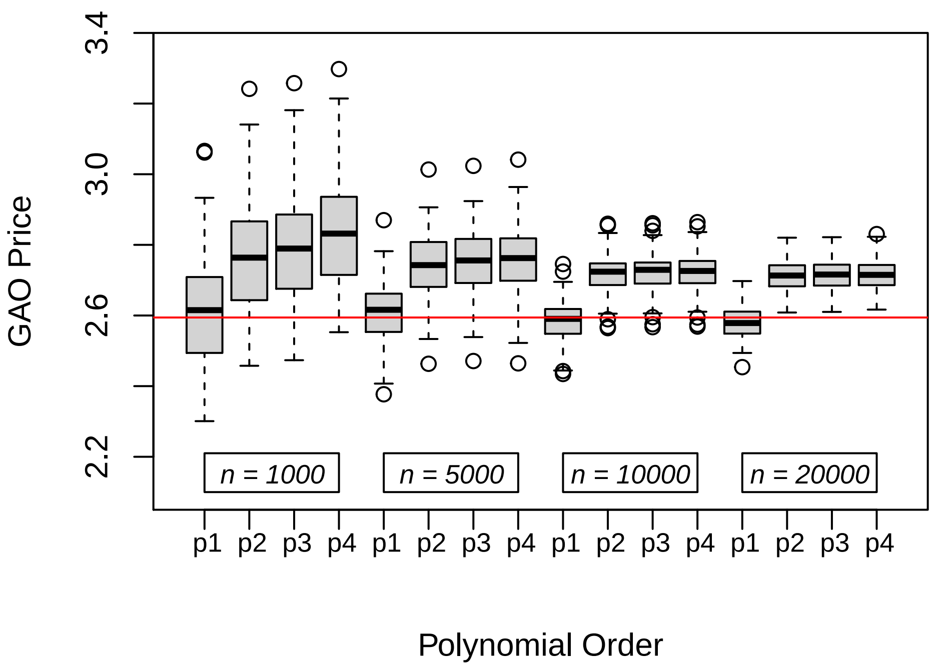

FIG. 8. Box-plots relative to the 100 GAO price estimates obtained by considering different numbers of outer scenarios and different polynomial orders. The horizontal red line refers to the benchmark value obtained through nested simulations (20000 × 20000 trajectories). GAO subscribed by an individual aged $x = 55$ today with maturity $T = 10$.

Once again, from Table 18 and Figure 8, we can appreciate the good performance of the LSMC approach. In particular, we can see that increasing the number of outer scenarios helps in decreasing the variability of the LSMC estimates. Moreover, we can notice that, as in Section 3, increasing the polynomial order is not a profitable choice due to the higher number of regressors used without increasing sufficiently the number of outer trajectories.

5. Conclusions

In this paper we faced the problem of approximating future annuity values. We proposed a methodology, based on the LSMC approach, which turned out to be quite accurate. Our results highlight the need of developing reliable actuarial models able to capture the source of risk arising from longevity and interest rate. These are not negligible aspects, especially for solvency purposes. Further, the paper has shown many contexts in which the valuation of future annuity contracts plays a relevant role, and hence where the LSMC algorithm helps in reducing the computational demand by preserving at the same time the accuracy of any desired quantities. The LSMC method turned out to be quite flexible to accomodate any computational framework withouth increasing the computational complexity.

APPENDIX A

Least-Squares Monte Carlo with Control Variates

Among the variance reduction techniques, the control variates method is the most effective approach to improve the efficiency of Monte Carlo simulation (see Glasserman, 2004). The idea is to exploit the information about the errors in estimates of known quantities to reduce the error in an estimate of an unknown quantity. It consists in replacing the random variable of interest, Y, with a new random variable Z which has the same expectation. In particular, we have the new random variable Z defined as

$$Z = Y - \theta \left(X - \mathbb{E}\left[X \right] \right),$$

where X is the control variate, θ is a (real-valued) parameter, and the term $X - \mathbb{E}[X]$ serves as a control in estimating $\mathbb{E}[Y]$. Then, an estimator of $\mathbb{E}[Z]$ can be its sample mean

$$\bar{Z}(\theta) = \frac{1}{n} \sum_{i=1}^{n} \left(Y_i - \theta \left(X_i - \mathbb{E}\left[X \right] \right) \right). \tag{A1}$$

It can be shown that the variance of the estimator defined in Equation (A1) is minimized if

$$\theta = \frac{\mathrm{Cov}\left[Y,\, X \right]}{\mathrm{Var}\left[X \right]}.$$

A similar idea can be exploited also in a LSMC framework as suggested by Rasmussen (2005), and further empirically applied by Mozgin (2010), where a new random variable with the same conditional expectation needs to be identified.

Control Variate: the GAPC family

Let us consider the mathematical framework defined in Section 3 where only mortality risk is taken into account, and denote with $A^{(i)}_{x+T}(T)$ the value of the annuity contract referring to the i-th outer scenario obtained by averaging across the few inner simulations. Then, we define the new set of observations as

$$\left\{A^{(i)}_{x+T}(T) - \theta\left(M^{(i)}_{x+T}(T,l) - \mathbb{E}\left[M^{(i)}_{x+T}(T,l) \mid \mathbf{z}_T\right]\right)\right\}_{i=1,\dots,n},$$

where $\mathbf{z}_T$ is the state-vector, and $M_{x+T}(T,l)$ is the control variate defined as follows

$$M_{x+T}(T,l) = \sum_{h=0}^{l-1} m_{x+T+h,T+h}.$$

In what follows, we compute the conditional expectation of the control variate which has then been used to obtain the numerical results in Section 3. In particular, we consider the class of Generalized-Age-Period-Cohort stochastic mortality models where we know that, under a Poisson setting, the logs of mortality rates are modelled through the following equation:

$$\log m_{x;t} = \alpha_x + \sum_{i=1}^{N} \beta^{(i)}_x \kappa^{(i)}_t + \beta^{(0)}_x \gamma_{t-x}, \tag{A2}$$

where α_x is a static-age function, $N \geq 0$ is an integer indicating the number of age-period terms describing the mortality trends, with each time index $\kappa^{(i)}_t$ contributing in specifying the mortality trend and $\beta^{(i)}_x$ modulating its effect across ages, and γ_{t-x} accounts for the cohort effect with $\beta^{(0)}_x$ modulating its effect across ages. We assume that the period indexes follow a multivariate random walk with drift as in Cairns et al. (2006, 2011), Haberman and Renshaw (2011) and Lovász (2011), i.e.

$$\boldsymbol{\kappa}_t = \boldsymbol{\delta} + \boldsymbol{\kappa}_{t-1} + \boldsymbol{\epsilon}_t, \qquad \boldsymbol{\kappa}_t = \begin{bmatrix} \kappa^{(1)}_t \\ \kappa^{(2)}_t \\ \vdots \\ \kappa^{(N)}_t \end{bmatrix}, \qquad \boldsymbol{\epsilon}_t \sim \mathrm{N}(\mathbf{0}, \boldsymbol{\Sigma}),$$

where $\boldsymbol{\delta}$ is the vector of drift parameters, and $\boldsymbol{\Sigma}$ is the $N \times N$ variance-covariance matrix of the multivariate white noise $\boldsymbol{\epsilon}_t$.

Hence, we have that, conditional on $\boldsymbol{\kappa}_T$,

$$\boldsymbol{\kappa}_{T+h} \mid \boldsymbol{\kappa}_T \sim \mathrm{N}(h\boldsymbol{\delta} + \boldsymbol{\kappa}_T, h\boldsymbol{\Sigma}).$$

Our first objective is to determine the distribution of $m_{x+h;T+h} \mid \mathbf{z}_T$, where $\mathbf{z}_T = [\boldsymbol{\kappa}_T, \gamma_{T-x}]$ is the state-vector. To this end, we define the vectors

$$\boldsymbol{\beta}_{x+h} = \begin{bmatrix} \beta^{(1)}_{x+h} \\ \beta^{(2)}_{x+h} \\ \vdots \\ \beta^{(N)}_{x+h} \end{bmatrix}, \qquad \boldsymbol{\mu}_h = \begin{bmatrix} \kappa^{(1)}_T + h\delta^{(1)} \\ \kappa^{(2)}_T + h\delta^{(2)} \\ \vdots \\ \kappa^{(N)}_T + h\delta^{(N)} \end{bmatrix},$$

and the variance-covariance matrix

$$\boldsymbol{\Sigma}_h = \begin{bmatrix} \sigma^2_{\epsilon_1} & \rho_{\epsilon_1\epsilon_2}\sigma_{\epsilon_1}\sigma_{\epsilon_2} & \dots & \rho_{\epsilon_1\epsilon_N}\sigma_{\epsilon_1}\sigma_{\epsilon_N} \\ \rho_{\epsilon_1\epsilon_2}\sigma_{\epsilon_1}\sigma_{\epsilon_2} & \sigma^2_{\epsilon_2} & \dots & \rho_{\epsilon_2\epsilon_N}\sigma_{\epsilon_2}\sigma_{\epsilon_N} \\ \vdots & \vdots & \ddots & \vdots \\ \rho_{\epsilon_1\epsilon_N}\sigma_{\epsilon_1}\sigma_{\epsilon_N} & \rho_{\epsilon_2\epsilon_N}\sigma_{\epsilon_2}\sigma_{\epsilon_N} & \dots & \sigma^2_{\epsilon_N} \end{bmatrix} \cdot h.$$

Therefore, we can write

$$m_{x+h;T+h} \mid \mathbf{z}_T = e^{\alpha_{x+h}+\boldsymbol{\beta}^\intercal_{x+h}\cdot\boldsymbol{\mu}_h+\beta^{(0)}_{x+h}\gamma_{T-x}} \mid \mathbf{z}_T \sim \exp\left\{\mathrm{N}\left(\alpha_{x+h}+\boldsymbol{\beta}^\intercal_{x+h}\cdot\boldsymbol{\mu}_h+\beta^{(0)}_{x+h}\gamma_{T-x}\ ,\ \boldsymbol{\beta}^\intercal_{x+h}\boldsymbol{\Sigma}_h\boldsymbol{\beta}_{x+h}\right)\right\},$$

and so, we have that $m_{x+h;T+h} \mid \mathbf{z}_T$ is log-normally distributed

$$m_{x+h;T+h} \mid \mathbf{z}_T \sim \mathrm{LN}\left(\alpha_{x+h}+\boldsymbol{\beta}^\intercal_{x+h}\cdot\boldsymbol{\mu}_h+\beta^{(0)}_{x+h}\gamma_{T-x}\ ,\ \boldsymbol{\beta}^\intercal_{x+h}\boldsymbol{\Sigma}_h\boldsymbol{\beta}_{x+h}\right). \tag{A3}$$

It follows that

$$\mathbb{E}\left[m_{x+h;T+h} \mid \mathbf{z}_T\right] = e^{\alpha_{x+h}+\boldsymbol{\beta}^\intercal_{x+h}\cdot\boldsymbol{\mu}_h+\beta^{(0)}_{x+h}\gamma_{T-x}+\frac{1}{2}\boldsymbol{\beta}^\intercal_{x+h}\boldsymbol{\Sigma}_h\boldsymbol{\beta}_{x+h}}.$$

Considering the control variate

$$M_{x+T}(T,l) = \sum_{h=0}^{l-1} m_{x+T+h,T+h},$$

we have that its conditional expectation can be easily computed as

$$\begin{aligned}\mathbb{E}\left[M_{x+T}(T,l) \mid \mathbf{z}_T\right] &= \mathbb{E}\left[\sum_{h=0}^{l-1} m_{x+h;T+h} \mid \mathbf{z}_T\right] = m_{x;T} + \sum_{h=1}^{l-1}\mathbb{E}\left[m_{x+h;T+h} \mid \mathbf{z}_T\right] \\ &= m_{x;T} + \sum_{h=1}^{l-1} e^{\alpha_{x+h}+\boldsymbol{\beta}^\intercal_{x+h}\cdot\boldsymbol{\mu}_h+\beta^{(0)}_{x+h}\gamma_{T-x}+\frac{1}{2}\boldsymbol{\beta}^\intercal_{x+h}\boldsymbol{\Sigma}_h\boldsymbol{\beta}_{x+h}}.\end{aligned}$$

Concerning the optimal level of θ, Rasmussen (2005) suggests to eventually estimate the second and cross-product moments through a linear combination of basis functions. However, in our numerical experiments we have fixed θ at a sub-optimal level.

APPENDIX B

The Wang Transform

The Wang Transform method consists essentially in distorting the cumulative distribution of a random variable Y. This yields a new risk-adjusted cumulative distribution of cash-flows that can be discounted at the risk-free rate. Specifically, Wang (2000) defines the following risk-adjusted distribution, that we take as risk-neutral one

$$\tilde{F}_Y(y) = \Phi\left[\Phi^{-1}(F_Y(y)) - \lambda\right], \tag{B1}$$

where $F_Y(y)$ is the CDF of the random variable Y under the physical measure $\mathbb{P}$, Φ is the CDF of a standard normal random variable, and λ is the risk premium.

Accordingly to Lin and Cox (2005), in the context of longevity risk transfer, the Wang transform in Equation (B1) can be explicitly written as

$$\tilde{F}_{T(x,0)}(i) = \Phi\left[\Phi^{-1}\left(F_{T(x,0)}(i)\right) - \lambda\right],$$

where $T(x,0)$ is the lifetime of a person aged x at time 0. The last equation can also be written as

$$_i\tilde{q}_{x,0} = \Phi\left[\Phi^{-1}\left(_iq_{x,0}\right) - \lambda\right], \tag{B2}$$

where $_iq_{x,0}$ is the probability that a person aged x at time 0 dies before age $x+i$, $i = 1, 2, \ldots$.

In bulk annuities, the market price of risk $\lambda > 0$, that we assume constant over time, reflects the level of both systematic and firm-specific unhedgeable longevity risk assumed by the insurer.

We can determine λ from a longevity security, so that at time 0 the price of the security is the discounted expected value under the transformed probability $_i\tilde{p}_{x,0} = 1 - {_i\tilde{q}_{x,0}}$. For instance, the price of an immediate life annuity contract for an individual aged x at time $t = 0$ would be

$$a_{x;0} = \sum_{i=1}^{\omega-x} e^{-ri} \cdot {_i\tilde{p}_{x,0}} = \sum_{i=1}^{\omega-x} e^{-ri} \cdot \left(1 - \Phi\left[\Phi^{-1}\left(_iq_{x,0}\right) - \lambda\right]\right). \tag{B3}$$

REFERENCES

Ayşe Arık, Yeliz Yolcu-Okur, Şule Şahin, and Ömür Uğur. Pricing pension buy-outs under stochastic interest and mortality rates. *Scandinavian Actuarial Journal*, 2018 (3):173–190, 2018. doi: 10.1080/03461238.2017.1328370. URL https://doi.org/10.1080/03461238.2017.1328370.

Laura Ballotta and Steven Haberman. Valuation of guaranteed annuity conversion options. *Insurance: Mathematics and Economics*, 33(1):87–108, 2003. ISSN 0167-6687. doi: https://doi.org/10.1016/S0167-6687(03)00146-X. URL https://www.sciencedirect.com/science/article/pii/S016766870300146X.

Laura Ballotta and Steven Haberman. The fair valuation problem of guaranteed annuity options: The stochastic mortality environment case. *Insurance: Mathematics and Economics*, 38(1):195–214, 2006. ISSN 0167-6687. doi: https://doi.org/10.1016/j.insmatheco.2005.10.002. URL https://www.sciencedirect.com/science/article/pii/S0167668705001435.

Daniel Bauer and Hongjun Ha. A least-squares monte carlo approach to the calculation of capital requirements. 2013.

Enrico Biffis. Affine processes for dynamic mortality and actuarial valuations. *Insurance: Mathematics and Economics*, 37(3):443–468, 2005. ISSN 0167-6687. doi: https://doi.org/10.1016/j.insmatheco.2005.05.003. URL https://www.sciencedirect.com/science/article/pii/S0167668705000600.

Enrico Biffis and Pietro Millossovich. The fair value of guaranteed annuity options. *Scandinavian Actuarial Journal*, 2006(1):23–41, 2006. doi: 10.1080/03461230500462204. URL https://doi.org/10.1080/03461230500462204.

David Blake, Andrew Cairns, Guy Coughlan, Kevin Dowd, and Richard MacMinn. The new life market. *Journal of Risk and Insurance*, 80(3):501–558, 2013. doi: https://doi.org/10.1111/j.1539-6975.2012.01514.x. URL https://onlinelibrary.wiley.com/doi/abs/10.1111/j.1539-6975.2012.01514.x.

M. Martin Boyer and Lars Stentoft. If we can simulate it, we can insure it: An application to longevity risk management. *Insurance: Mathematics and Economics*, 52(1):35–45, 2013. ISSN 0167-6687. doi: https://doi.org/10.1016/j.insmatheco.2012.10.003. URL https://www.sciencedirect.com/science/article/pii/S0167668712001175.

Phelim Boyle and Mary Hardy. Guaranteed annuity options. *ASTIN Bulletin*, 33(2): 125–152, 2003. doi: 10.1017/S0515036100013404.

Andrew J. G. Cairns, David Blake, and Kevin Dowd. A two-factor model for stochastic mortality with parameter uncertainty: Theory and calibration. *Journal of Risk and Insurance*, 73(4):687–718, 2006. doi: https://doi.org/10.1111/j.1539-6975.2006.00195.x. URL https://onlinelibrary.wiley.com/doi/abs/10.1111/j.1539-6975.2006.00195.x.

Andrew J. G. Cairns, David Blake, Kevin Dowd, Guy D. Coughlan, David Epstein, Alen Ong, and Igor Balevich. A quantitative comparison of stochastic mortality models using data from england and wales and the united states. *North American Actuarial Journal*, 13(1):1–35, 2009. doi: 10.1080/10920277.2009.10597538. URL https://doi.org/10.1080/10920277.2009.10597538.

Andrew J.G. Cairns. Modelling and management of longevity risk: Approximations to survivor functions and dynamic hedging. *Insurance: Mathematics and Economics*, 49(3):438–453, 2011. ISSN 0167-6687. doi: https://doi.org/10.1016/j.insmatheco.2011.06.004. URL https://www.sciencedirect.com/science/article/pii/S0167668711000771.

Andrew J.G. Cairns, David Blake, Kevin Dowd, Guy D. Coughlan, David Epstein, and Marwa Khalaf-Allah. Mortality density forecasts: An analysis of six stochastic mortality models. *Insurance: Mathematics and Economics*, 48(3):355–367, 2011. ISSN 0167-6687. doi: https://doi.org/10.1016/j.insmatheco.2010.12.005. URL https://www.sciencedirect.com/science/article/pii/S0167668710001484.

Michel Denuit. Comonotonic approximations to quantiles of life annuity conditional expected present value. *Insurance: Mathematics and Economics*, 42(2):831–838,

2008. ISSN 0167-6687. doi: https://doi.org/10.1016/j.insmatheco.2007.09.006. URL https://www.sciencedirect.com/science/article/pii/S0167668707000984.

Kevin Dowd, David Blake, and Andrew J. G. Cairns. A computationally efficient algorithm for estimating the distribution of future annuity values under interest-rate and longevity risks. *North American Actuarial Journal*, 15(2):237–247, 2011. doi: 10.1080/10920277.2011.10597619. URL https://doi.org/10.1080/10920277.2011.10597619.

Paul Glasserman. *Monte Carlo methods in financial engineering*. Springer, New York, 2004. ISBN 0387004513 9780387004518 1441918221 9781441918222. URL http://www.amazon.com/Financial-Engineering-Stochastic-Modelling-Probability/dp/0387004513/ref=pd_sim_b_68?ie=UTF8&refRID=1AN8JXSDGMEV2RPHFC2A.

Steven Haberman and Arthur Renshaw. A comparative study of parametric mortality projection models. *Insurance: Mathematics and Economics*, 48(1):35–55, 2011. ISSN 0167-6687. doi: https://doi.org/10.1016/j.insmatheco.2010.09.003. URL https://www.sciencedirect.com/science/article/pii/S0167668710001022.

Tom Hoedemakers, Grzegorz Darkiewicz, and Marc Goovaerts. Approximations for life annuity contracts in a stochastic financial environment. *Insurance: Mathematics and Economics*, 37(2):239–269, 2005. ISSN 0167-6687. doi: https://doi.org/10.1016/j.insmatheco.2005.02.003. URL https://www.sciencedirect.com/science/article/pii/S0167668705000144. Papers presented at the 8th IME Conference, Rome, 14-16 June 2004.

Nan Li and Ronald Lee. Coherent mortality forecasts for a group of populations: An extension of the lee-carter method. *Demography*, 42(3):575–594, 2005. ISSN 00703370, 15337790. URL http://www.jstor.org/stable/4147363.

Yijia Lin and Samuel H. Cox. Securitization of mortality risks in life annuities. *The Journal of Risk and Insurance*, 72(2):227–252, 2005. ISSN 00224367, 15396975. URL http://www.jstor.org/stable/3519949.

Yijia Lin, Tianxiang Shi, and Ayşe Arik. Pricing buy-ins and buy-outs. *Journal of Risk and Insurance*, 84(S1):367–392, 2017. doi: https://doi.org/10.1111/jori.12159. URL https://onlinelibrary.wiley.com/doi/abs/10.1111/jori.12159.

Xiaoming Liu. Annuity uncertainty with stochastic mortality and interest rates. *North American Actuarial Journal*, 17(2):136–152, 2013. doi: 10.1080/10920277.2013.795481. URL https://doi.org/10.1080/10920277.2013.795481.

Francis A. Longstaff and Eduardo S. Schwartz. Valuing american options by simulation: A simple least-squares approach. *The Review of Financial Studies*, 14(1):113–147, 06 2001. ISSN 0893-9454. doi: 10.1093/rfs/14.1.113. URL https://doi.org/10.1093/rfs/14.1.113.

Enrico Lovász. Analysis of finnish and swedish mortality data with stochastic mortality models. *European Actuarial Journal*, 1:259–289, 2011. doi: 10.1007/s13385-011-0039-8. URL https://doi.org/10.1007/s13385-011-0039-8.

Victor Mozgin. Optimized least-squares monte carlo for measuring counterparty credit exposure of american-style options. 2010.

S. E. Oppers, K. Chikada, K. Chikada, F. Eich, P. Imam, J. Kiff, M. Kisser, M. Soto, and T. Sun. Global Financial Stability Report. The Financial Impact of Longevity Risk. *IMF*, 4, 2012.

N. S. Rasmussen. Control variates for monte carlo valuation of american options. *Journal of Computational Finance*, 9, 2005.

Shaun S. Wang. A class of distortion operators for pricing financial and insurance risks. *The Journal of Risk and Insurance*, 67(1):15–36, 2000. ISSN 00224367, 15396975. URL http://www.jstor.org/stable/253675.